The Astrophysical Journal Letters, 884:L9 (6pp), 2019 October 10 https://doi.org/10.3847/2041-8213/ab46c3

Evidence of Nonluminous Matter in the Center of M62

Federico Abbate[1,2], Andrea Possenti[2,3], Monica Colpi[1,4,5], and Mario Spera[1,6,7,8,9]
[1] Dipartimento di Fisica "G. Occhialini," Università degli Studi Milano-Bicocca, Piazza della Scienza 3, I-20126 Milano, Italy; f.abbate@campus.unimib.it
[2] INAF—Osservatorio Astronomico di Cagliari, Via della Scienza, I-09047 Selargius (CA), Italy
[3] Dipartimento di Fisica, Università di Cagliari, SP Monserrato-Sestu, km 0.7, I-09042 Monserrato, Italy
[4] Istituto Nazionale di Fisica Nucleare, Sezione di Milano Bicocca, Piazza della Scienza 3, I-20126 Milano, Italy
[5] INAF—Osservatorio Astronomico di Brera, via Brera 28, I-20121 Milan, Italy
[6] Dipartimento di Fisica e Astronomia "G. Galilei," University of Padova, Vicolo dell'Osservatorio 3, I-35122 Padova, Italy
[7] INFN, Sezione di Padova, Via Marzolo 8, I-35131 Padova, Italy
[8] Department of Physics and Astronomy, Northwestern University, Evanston, IL 60208, USA
[9] Center for Interdisciplinary Exploration and Research in Astrophysics (CIERA), Evanston, IL 60208, USA
Received 2019 July 26; revised 2019 September 12; accepted 2019 September 23; published 2019 October 7

Abstract

Theoretical models suggest that intermediate-mass black holes (IMBHs) may form and reside in the centers of globular clusters. IMBHs are still elusive to observations, but the accelerations of pulsars may bring along a unique fingerprint of their presence. In this work, we focus on the pulsars in the globular cluster M62. Using the new distance of M62 obtained from *Gaia* observations, we find that the measured pulsars' accelerations suggest a central excess of mass in the range [1200, 6000] $M_\odot$, corresponding to [0.2, 1]% of the current total mass of the cluster. Our analysis cannot unambiguously discriminate between an IMBH or a system of stellar mass dark remnants of comparable total mass.

Unified Astronomy Thesaurus concepts: Intermediate-mass black holes (816); Millisecond pulsars (1062); Globular star clusters (656)

1. Introduction

Intermediate-mass black holes (IMBHs) are black holes with a mass between 10^2 and 10^5 $M_\odot$. They are considered the missing link between stellar black holes and supermassive black holes, and they may also be the seeds upon which supermassive black holes form (Volonteri 2010; Johnson & Haardt 2016; Latif & Ferrara 2016; Mezcua 2017). Theoretical models suggest that IMBHs can be found in dense stellar environments such as globular clusters (GCs; Bahcall & Ostriker 1975). In GCs, the high number of stellar collisions and gravitational encounters could favor the formation of IMBHs through repeated mergers of massive stars or stellar black holes segregated in the center (Miller & Hamilton 2002; Portegies Zwart & McMillan 2002; Gürkan et al. 2004; Portegies Zwart et al. 2004; Giersz et al. 2015). Alternatively, if the stellar black holes do not merge, they could form a massive subsystem in the cluster center that may mimic the effects of an IMBH (Breen & Heggie 2013a).

Studying the dynamics of stars and looking for signatures of accretion are two possible ways to reveal the presence of IMBHs in GCs. Both methods have been extensively applied to many Galactic GCs finding upper limits or tentative detections (McLaughlin et al. 2006; Noyola et al. 2008; van der Marel & Anderson 2010; Lützgendorf et al. 2013) that have been partially disputed (Baumgardt 2017; Tremou et al. 2018). Evidence of an IMBH in an extragalactic stellar cluster might have been found thanks to observations of a tidal disruption event (Lin et al. 2018).

Additional evidence toward the presence of an IMBH in a GC can come from the accelerations of the cluster's pulsars, which can be measured thanks to the Doppler effect and the very stable periodic emission (Kızıltan et al. 2017a, 2017b; Perera et al. 2017a, 2017b; Abbate et al. 2018).

In this Letter, we focus on the GC M62, also known as NGC 6266. Using the observed velocity dispersion and surface brightness profiles, McNamara et al. (2012) could not exclude the presence of an IMBH while Lützgendorf et al. (2013) showed that this cluster may contain an IMBH with a mass of 2000 $M_\odot$. The latter claim has been recently contested by Baumgardt et al. (2019), who showed that the observations are better matched by theoretical models that do not include an IMBH. Furthermore, in a search for radio signatures of accretion from a hypothetical central IMBH, Tremou et al. (2018) failed in the detection. Instead, they posed an upper limit to the IMBH mass at 1130 $M_\odot$. M62 contains six known millisecond pulsars (MSPs), all of which are in binary systems (D'Amico et al. 2001; Possenti et al. 2003; Lynch et al. 2012). Three pulsars are located very close to the center of the cluster (∼0.1 pc). As such, they may bring along crucial information about the possible presence of a central IMBH. In this work, we use the accelerations of the pulsars in M62 to look for deviations from the published density profile of the cluster and we investigate whether this deviation can be attributed to an IMBH or a central nonluminous system.

2. Methods

Millisecond pulsars are excellent tools to probe the dynamics of M62 thanks to their very stable rotation. The high stability allows us a high-accuracy measure of the rotational period derivatives, which, in turn, are linked to the pulsars' accelerations (and derivatives) by the Doppler effect. Furthermore, due to mass segregation (Spitzer 1987), pulsars are usually located close to the center of the cluster giving us insights into the mass distribution in the cluster's innermost regions.

The line-of-sight acceleration of a pulsar is related to its rotational period derivative $\dot{P}$ by the equation

$$\left(\frac{\dot{P}}{P}\right)_{\rm meas} = \left(\frac{\dot{P}}{P}\right)_{\rm int} + \frac{a_c}{c} + \frac{a_{\rm g}}{c} - \frac{\mu^2 D}{c}, \quad (1)$$

where $(\dot{P}/P)_{\rm int}$ is the spin-down caused by magnetic dipole braking, a_c/c is the acceleration along the line of sight caused by the gravitational potential of the GC, $a_{\rm g}/c$ is the relative acceleration of the cluster with respect to the solar system in the gravitational potential of the Galaxy, $\mu^2 D/c$ is the centrifugal acceleration caused by the proper motion of the pulsars called the Skhlovskii effect (Shklovskii 1970), μ is the proper motion of the pulsar, D is the distance of the cluster, and c is the speed of light.

The contribution of the Shklovskii effect for the pulsars in M62 can be measured assuming the proper motion of the GC ($\mu = 5.79$ mas yr^{-1}; *Gaia* Collaboration et al. 2018) multiplied by c. This means we get a typical acceleration of $\sim 10^{-10}$ m s^{-2}. The contribution of the gravitational potential of the Galaxy at the GC's Galactic coordinates ($l_{\rm g} = 353.^{\circ}574$, $b_{\rm g} = 7.^{\circ}318$), derived from the Galactic potential model of Kuijken & Gilmore (1989), is (Nice & Taylor 1995)

$$a_{\rm g} = -\cos(b_{\rm g})\left(\frac{\Theta_0^2}{R_0}\right)\left[\cos(l_{\rm g}) + \frac{\beta}{\sin^2(l_{\rm g}) + \beta^2}\right], \quad (2)$$

where $R_0 = 8178 \pm 12_{\rm stat} \pm 22_{\rm sys}$ kpc is the distance of the Galactic center (Gravity Collaboration et al. 2019), $\Theta_0 = 240 \pm 8$ km s^{-1} (Sharma et al. 2014), and $\beta = (D/R_0)\cos(b_{\rm g}) - \cos(l_{\rm g})$. We obtain $a_{\rm g} \simeq 5 \times 10^{-10}$ m s^{-2}.

The intrinsic spin-down caused by magnetic dipole braking can vary from pulsar to pulsar. The average value can be estimated from the statistical distribution of intrinsic spin-down from the population of MSPs from the Galactic disk. For them the observed $(\dot{P}/P)_{\rm meas}$ is dominated by the intrinsic spin-down. Taking into account the population of Galactic MSPs (Manchester et al. 2005), Abbate et al. (2018) find that the contribution on the acceleration due to the intrinsic spin-down is of the order of 10^{-9} m s^{-2}.

The measured acceleration, $c(\dot{P}/P)_{\rm meas}$, of the pulsars in M62 in absolute value varies from 3×10^{-9} m s^{-2} for pulsar C to 3×10^{-8} m s^{-2} for pulsar B. This means that the dominant contribution is due to the acceleration caused by the gravitational potential of the cluster, a_c. This acceleration can be estimated directly using formulas derived from the density distribution of the cluster, usually considered to be a King profile (King 1962). These equations, however, depend on the distance of the pulsar from the center of the cluster along the line of sight. This quantity is not directly measurable from the observations and is therefore an unknown.

To calculate analytically a_c and search for the gravitational effects of an IMBH we have to fit for the structural parameters of the GC together with the line-of-sight distances of the pulsars. We use a Markov Chain Monte Carlo (MCMC) code first introduced in Prager et al. (2017) and further developed in Abbate et al. (2018). This code uses the information derived from the position of pulsars in the plane of the sky and their acceleration along the line of sight to find the best match for (i) the structural parameters of the cluster, (ii) the position along the line of sight of each pulsar, and (iii) the mass of a dark massive object, $M_\bullet$, which corresponds to an IMBH if $M_\bullet > 10^2\,M_\odot$. As structural parameters, we use the core radius r_c and the central mass density ρ_0. Alternatively to the central density, the one-dimensional central velocity dispersion, σ_c, can be used. The latter has the advantage of being measurable in observations and is linked to the other two parameters by the equation (Binney & Tremaine 2008)

$$\sigma_c = \sqrt{\frac{4\pi G \rho_0 r_c^2}{9}}. \quad (3)$$

An additional parameter that is used by the MCMC code is the mass segregation parameter α. This is linked to the column number density profile of the pulsars by the following formula Lugger et al. (1995):

$$n(x_\perp) = n_0(1 + x_\perp^2)^{\alpha/2}, \quad (4)$$

where n_0 is the central number density, and $x_\perp$ is the distance from the center in the plane of the sky in units of core radii, defined as $x_\perp = R_\perp/r_c$. The mass segregation parameter α is related to the mass of the pulsars by the formula $\alpha = 1$–$3q$, where q is the ratio between the mass of the pulsar $M_{\rm p}$ and the mass of the stellar population that dominates the dynamics in the cluster ($q = M_{\rm p}/M_*$). If pulsars have the same mass as the dominant mass class we obtain $\alpha = -2$, which is the value for the single-mass analytical King model (King 1962). In typical GCs $\alpha \simeq -3$ (Prager et al. 2017; Abbate et al. 2018). We take the prior on this parameter to be a Gaussian centered on -3 with a dispersion of 0.5.

We use the α parameter to estimate the probability that a pulsar will have a given line-of-sight distance from the center of the cluster. Furthermore, we assume that the GC is spherical and that the distribution of pulsars along the line of sight is the same as the number density profile along the directions on the plane of the sky.

Table 1
Properties of the GC M62 Using Optical Data

Parameter	Value	Reference
Stellar mass	$6.74 \pm 0.05 \times 10^5\,M_\odot$	1
Distance	6400 ± 180 pc	2
Core radius	0.36 pc	1
Velocity dispersion		
Radial	15.0 ± 1.1 km s^{-1}	3
Proper motion	15.3 ± 0.4 km s^{-1}	4

References. (1) Baumgardt & Hilker (2018); (2) Baumgardt et al. (2019); (3) Kamann et al. (2018); (4) Watkins et al. (2015)

3. Observational Parameters

The GC M62 has been observed at different wavelengths over the years in order to measure the parameters of the cluster. The properties important for the present work are shown in Table 1.

The most recent distance estimate obtained through *Gaia* observations (Baumgardt et al. 2019) is 6400 ± 180 pc. This value is smaller than the value found in Harris (1996) (2010 edition) which was 6800 pc. Throughout the paper we will use the new distance estimated by Baumgardt et al. (2019).

The core radius can be derived from the luminosity density profile with a single-mass King model (King 1962). Using *Hubble Space Telescope* observations, Miocchi et al. (2013)

found $15\farcs4 \pm 0\farcs6$, which corresponds to 0.48 ± 0.02 pc. In contrast, recent *N*-body simulations that match the surface density, the velocity dispersion, and the mass function of M62 suggest a smaller core radius of about 0.36 pc (Baumgardt & Hilker 2018).[10]

Using radial velocity measurements, Kamann et al. (2018) obtained a value of the central velocity dispersion of 15.0 ± 1.1 km s^{-1}. Using proper motion data, Watkins et al. (2015) estimated a value of 0.504 ± 0.004 mas yr^{-1}, corresponding to that converted to km s^{-1} using the newly determined distance becomes 15.3 ± 0.4 km s^{-1}.

Further information about the dynamical structure of the cluster can be gathered from radio observations of the pulsars. The ephemerides of the pulsars in M62 are taken from Lynch et al. (2012) and include information on the position of the pulsars in the plane of the sky, their rotational periods (and higher time derivatives), and the binary parameters. Using the position of the center of gravity as given in Miocchi et al. (2013), pulsars B, E, and F are at about 4″ from the cluster's center. At a distance of 6400 pc (Baumgardt 2017) this corresponds to about 0.1 pc. This distance is comparable with that of the innermost bin in the velocity dispersion profile presented by Watkins et al. (2015). The accelerations of these three pulsars are crucial to get insights into the central cluster's mass distribution.

4. Results

To perform the fit for the IMBH we need to assume some priors on the parameters. We use the most precise values determined from optical observations (see Section 3). We take the velocity dispersion measured with proper motion data and the core radius as estimated in Baumgardt & Hilker (2018) and the distance measured with *Gaia* data. The priors for the parameters are Gaussians centered around those values and with the quoted uncertainty as the standard deviation. For the core radius the standard deviation was chosen to be 0.01 pc (the same fractional uncertainty as the distance). The corner plot of the core radius, central density, and central dark object mass is shown in Figure 1. The comparison between the measured accelerations of the pulsars and the ones predicted by the best-fitting model are shown in Figure 2. Only the innermost three pulsars are shown as they are the most affected by the presence of the central object. The posterior distribution function for the mass of the central dark object in logarithmic units is shown in Figure 3. We find that an excess mass of 3900 $M_\odot$ is needed in the center to explain the measured pulsar accelerations. The 68% interval is (1200, 6600) $M_\odot$. The posterior distribution becomes compatible with the case of no IMBH ($M_\bullet < 10^2\,M_\odot$) if we consider the 95% interval. This excess is on top of the mass distribution estimated for a single-mass King model derived from the observed optical parameters and is located within 0.2 pc (the distance from the center of the innermost pulsar, F). The central mass density converges to $(3.1 \pm 0.2) \times 10^5\,M_\odot$ pc^{-3}. This value is almost twice than what was estimated through *N*-body simulations in Baumgardt & Hilker (2018), which is $1.6 \times 10^5\,M_\odot$ pc^{-3}. This means that an excess of mass in the center is needed to explain the accelerations of the pulsars. This also is apparent in the lower left panel of the corner plot in Figure 1 where we see that if there is no IMBH, the central density must increase in order to compensate for the missing mass.

To test the nature of the excess of mass, we measure the central mass-to-light ratio. First, we transform the central density in a surface mass density by multiplying it by $2r_c$ (Freire et al. 2005). This is compared with the surface

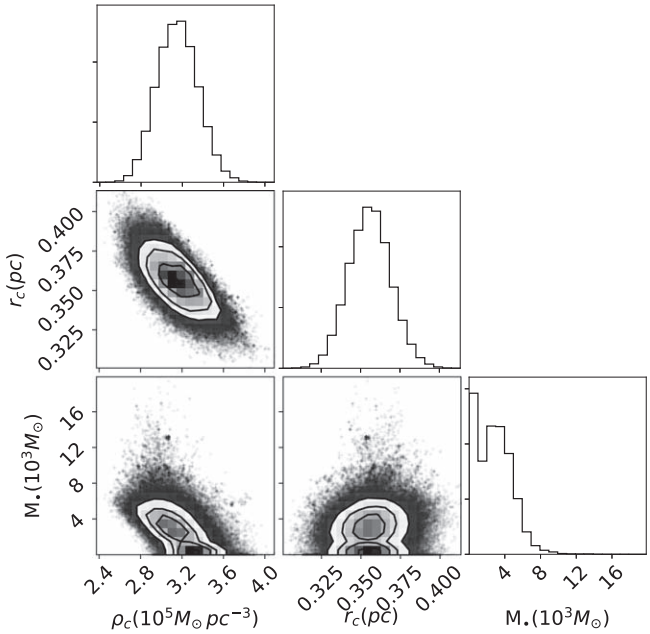

Figure 1. Corner plot showing the posterior distribution of the central density, the core radius, and the mass of the central dark object.

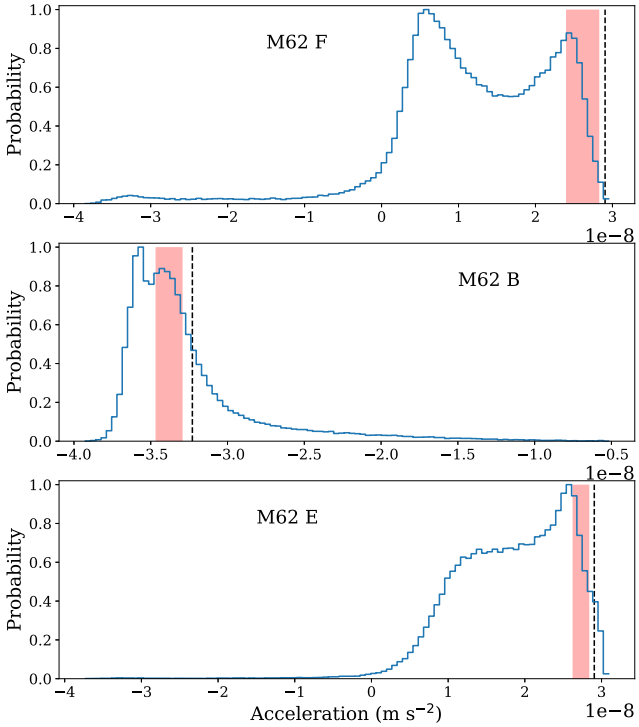

Figure 2. Posterior distribution for the accelerations of the pulsars F, B, and E, the three pulsars closer to the center. The dashed line shows the measured value of $\dot{P}/P$, and the red shaded area is the 1σ interval of the cluster acceleration after removing the Galactic contribution, the Shkolvskii effect, and the intrinsic spin-down.

[10] For a complete list of structural parameters derived from *N*-body simulations for all known GCs see https://people.smp.uq.edu.au/HolgerBaumgardt/globular/parameter.html.

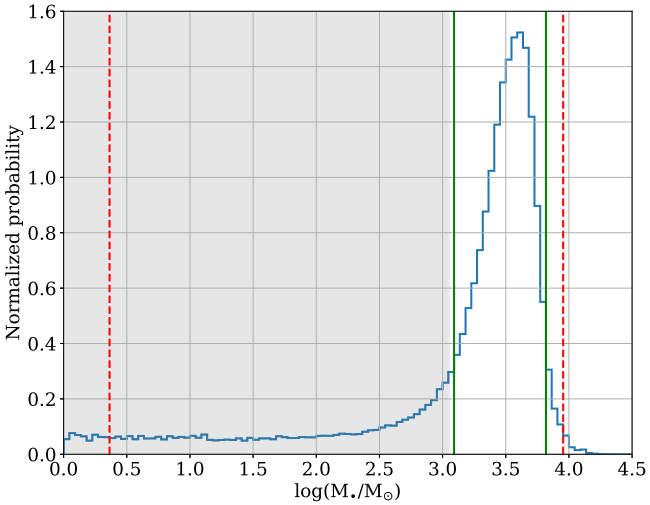

Figure 3. Posterior distribution function on the mass of the central dark object in logarithmic units. The green lines show the 68% interval, and the dashed red lines show the 95% interval. The shaded interval is the allowed IMBH mass range from Tremou et al. (2018). We assume a core radius of 0.36 pc as in Baumgardt & Hilker (2018).

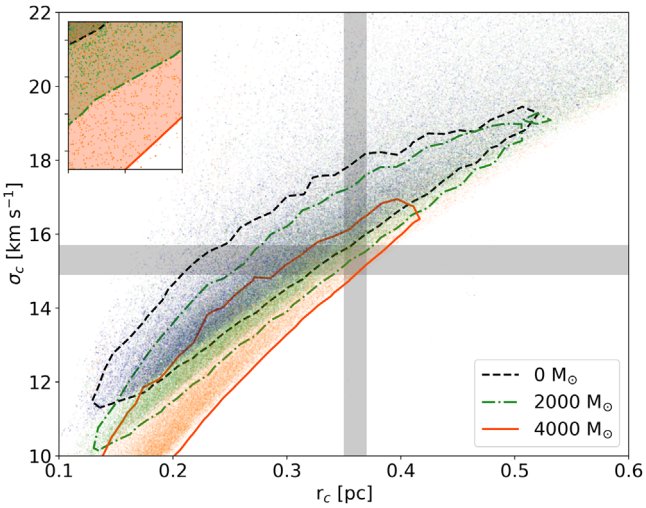

Figure 4. Contour plot of the posterior distribution of core radius and velocity dispersion as resulting from the MCMC fit. The shaded gray area shows the 1σ interval of the best determinations of core radius and velocity dispersion. The different sets represent fits with three values of IMBH mass: 0 $M_\odot$ (gray), 2000 $M_\odot$ (green), 4000 $M_\odot$ (orange). The colored lines show the 68% intervals of these distributions. The inset shows a zoom on the central shaded area.

brightness density measured in Noyola & Gebhardt (2006) and converted into solar luminosities per square parsec. The resulting central mass-to-light ratio and the 68% interval is $6.4^{+2.1}_{-0.7}\,M_\odot\,L_\odot^{-1}$. This value is much higher than what is seen at the cluster centers in *N*-body simulations of different GCs (see Figure 3 in Baumgardt 2017). Alternatively to an IMBH, the central excess of mass could be explained with a system of stellar dark remnants like massive white dwarfs, neutron stars, or black holes. A system of this kind could form in the first evolutionary phases of a GC and survive up until now if the host cluster has a sufficiently long half-mass relaxation time like M62 (∼1 Gyr; Breen & Heggie 2013b; Arca-Sedda 2016; Arca Sedda et al. 2018).

4.1. Uncertainties in the Optical Parameters

We have shown that the probability of finding a central excess of mass in M62 is quite high. To check that our finding is not affected by possible systematic errors on the values of the core radius and on the central velocity dispersion, we repeat the MCMC fit by setting the IMBH mass to fixed values, without assuming any priors on the core radius and on the velocity dispersion. Figure 4 shows the posterior distribution of the fits for three masses of IMBH, 0 $M_\odot$, 2000 $M_\odot$, and 4000 $M_\odot$. In the same plot we show, with the shaded area, the observed 1σ range for the core radius and velocity dispersion. In the case with no IMBH the shaded interval intersects the 68% interval of the posterior distribution only in a very small region (shown in the inset), but, as the mass of the IMBH increases, the region of intersection grows. However, if the real core radius is smaller than the measured one it could be possible to explain the observed pulsar accelerations without the need of an IMBH. The same is true if the true velocity dispersion is higher than what is measured. It is important to note also that in these cases where the IMBH is not needed, the mass-to-light ratio must remain at the same values.

To test the relation between the mass excess and the core radius and velocity dispersion of the cluster, we run the MCMC code, using two mock GCs; the first (second) with a core radius of 0.16 pc (0.58 pc) and a total mass of $9 \times 10^4\,M_\odot$ ($8.4 \times 10^5\,M_\odot$) simulated in Abbate et al. (2019). The simulations host IMBHs of different masses in the center. Here, we show the result of the smallest cluster in the case there is no IMBH in the core. We first run the code with a prior on r_c corresponding to the true value of 0.16 pc inferred from the simulated GC, and later we inject an erroneous value of r_c overestimated by 60% to 0.26 pc. This overestimation corresponds to the difference between the largest measured r_c for M62, 0.48 pc (Miocchi et al. 2013), and the value it should have to be compatible with no IMBH keeping the same velocity dispersion taken from Figure 4, that is, ∼0.3 pc. We extract six pulsars (using $\alpha = 3$), and measure their acceleration along the line of sight for the two cases.

Figure 5 shows the histograms of the posterior distributions of the central dark object mass from the mock GC. The distribution in orange, corresponding to the incorrect value of r_c, shows a peak at ∼3500 $M_\odot$ that is incompatible with 0 $M_\odot$ at the 3σ level, whereas the distribution in blue is consistent with the correct assumption of no IMBH, at the 1σ level.

We repeat the test using the simulation of the same GC with an IMBH of 1000 $M_\odot$ at the center and for the more massive GC with a core radius of 0.58 pc. The simulations of both clusters strongly support that an error in the determination of the cluster parameters can lead to an incorrect value of the mass of the IMBH.

5. Discussion

We have used the measured accelerations of the pulsars in M62 and the new distance estimate by *Gaia* to predict the existence of an excess of mass located within the central 4″ of M62. The existence of a concentration of nonluminous mass is confirmed by looking at the very high central mass-to-light ratio (∼6). The source of this dark mass excess could be a single IMBH of ∼3900 $M_\odot$ or a system of massive dark remnants segregated in the center of a similar total mass. This result is obtained strictly assuming the nominal values of the core radius and velocity dispersion from the latest optical observations (Watkins et al. 2015; Baumgardt & Hilker 2018).

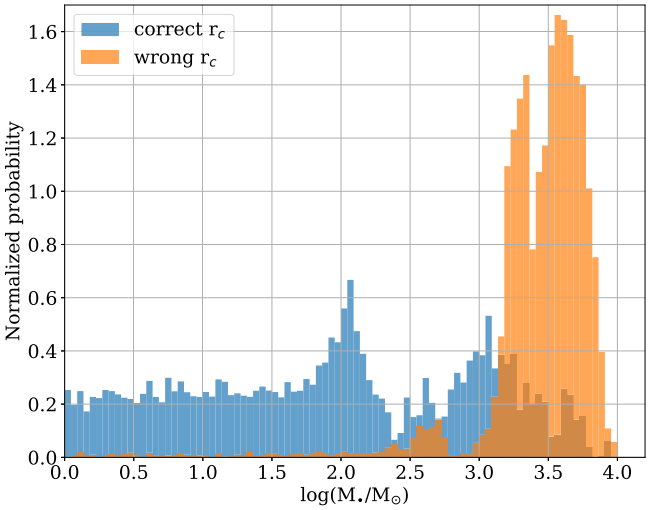

Figure 5. Posterior distributions of the mass of the central dark object resulting from a simulated GC with no such mass excess. Assuming the correct value of the core radius (blue histogram), the distribution is consistent with a null mass excess. Instead, assuming a core radius overestimated by 60% (orange histogram), the distribution indicates a mass excess of $\sim$3500 $M_\odot$, which is not present in the simulation.

We tested the dependence of the result from these assumptions and found important correlations between the aforementioned optical parameters and the mass of the IMBH resulting from the fit. Assuming a smaller core radius or a faster velocity dispersion would result in an IMBH of smaller mass.

We tested the correlation using simulated GCs of known parameters, and we confirmed that an alternate assumption on the core radius can mimic the necessity of an IMBH or can exclude its presence. Thus, more precise estimates of these parameters are needed to uniquely confirm the presence of an IMBH in the cluster.

The optical observations of M62 are compatible with an IMBH of a few thousand $M_\odot$ (McNamara et al. 2012) with a tentative claim of $\sim$2000 $M_\odot$ (Lützgendorf et al. 2013), which has been disputed in Baumgardt (2017). According to searches for accretion signatures (Tremou et al. 2018), there is an upper limit on the mass of the IMBH of 1130 $M_\odot$. From the results of our analysis, we cannot either confirm these claims or reduce the upper limits, but, using the published optical parameters of M62, we have found that $\sim$4000 $M_\odot$ of low-luminosity matter must be contained within the central 0.2 pc of the cluster. This "dark" matter can be composed of an unconstrained ratio between one or more IMBHs or a large number of nonluminous remnants of stellar origin.

Present-day clusters, with half-mass relaxation times $\gtrsim$1 Gyr, may have retained many stellar mass dark remnants in their centers (Breen & Heggie 2013b; Arca Sedda et al. 2018). Such subsystems can reach masses of 1000–10,000 $M_\odot$ for GCs born very massive (Arca-Sedda 2016). Arca Sedda et al. (2019) showed that M62-like GCs build up a subsystem of dark remnants in their center in about half of the authors' *N*-body realizations. Though highly speculative, some of these stellar remnants might be in the form of binary black holes, which are now observed as powerful gravitational-wave sources (Abbott et al. 2019). Furthermore, Ye et al. (2019) showed that the presence of a large number of black holes in the center of the clusters should drive out all of the MSPs found inside and would be incompatible with the observed set of pulsars. The stability of this system and the coexistence of stellar black holes and MSPs should be studied with dynamical simulations focused on this cluster.

Further observations of the cluster are necessary to find the source of the excess of mass. Optical observations will help to determine the structural parameters with higher precision, and radio observations will better constrain the accelerations of the pulsars and look for new pulsars possibly even closer to the center.

This work has been funded using resources from the research grant "iPeska" (PI: Andrea Possenti) funded under the INAF national call Prin-SKA/CTA approved with the Presidential Decree 70/2016. We acknowledge the "Accordo Quadro INAF-CINECA (2017)" and the CINECA-INFN agreement for the availability of high performance computing resources and support. M.C. acknowledges financial support by INFN under the grant Teongrav. M.S. acknowledges funding from the European Union's Horizon 2020 research and innovation programme under the Marie-Sklodowska-Curie grant agreement No. 794393.

ORCID iDs

Federico Abbate https://orcid.org/0000-0002-9791-7661
Monica Colpi https://orcid.org/0000-0002-3370-6152
Mario Spera https://orcid.org/0000-0003-0930-6930

References

Abbate, F., Possenti, A., Ridolfi, A., et al. 2018, MNRAS, 481, 627
Abbate, F., Spera, M., & Colpi, M. 2019, MNRAS, 487, 769
Abbott, B. P., Abbott, R., Abbott, T. D., et al. 2019, PhRvX, 9, 031040
Arca-Sedda, M. 2016, MNRAS, 455, 35
Arca Sedda, M., Askar, A., & Giersz, M. 2018, MNRAS, 479, 4652
Arca Sedda, M., Askar, A., & Giersz, M. 2019, MNRAS, submitted (arXiv:1905.00902)
Bahcall, J. N., & Ostriker, J. P. 1975, Natur, 256, 23
Baumgardt, H. 2017, MNRAS, 464, 2174
Baumgardt, H., & Hilker, M. 2018, MNRAS, 478, 1520
Baumgardt, H., Hilker, M., Sollima, A., & Bellini, A. 2019, MNRAS, 482, 5138
Binney, J., & Tremaine, S. 2008, Galactic Dynamics (2nd ed.; Princeton, NJ: Princeton Univ. Press)
Breen, P. G., & Heggie, D. C. 2013a, MNRAS, 436, 584
Breen, P. G., & Heggie, D. C. 2013b, MNRAS, 432, 2779
D'Amico, N., Lyne, A. G., Manchester, R. N., Possenti, A., & Camilo, F. 2001, ApJ, 548, L171
Freire, P. C. C., Hessels, J. W. T., Nice, D. J., et al. 2005, ApJ, 621, 959
Gaia Collaboration, Helmi, A., van Leeuwen, F., et al. 2018, A&A, 616, A12
Giersz, M., Leigh, N., Hypki, A., Lützgendorf, N., & Askar, A. 2015, MNRAS, 454, 3150
Gravity Collaboration, Abuter, R., Amorim, A., et al. 2019, A&A, 625, L10
Gürkan, M. A., Freitag, M., & Rasio, F. A. 2004, ApJ, 604, 632
Harris, W. E. 1996, AJ, 112, 1487
Johnson, J. L., & Haardt, F. 2016, PASA, 33, e007
Kamann, S., Husser, T. O., Dreizler, S., et al. 2018, MNRAS, 473, 5591
King, I. 1962, AJ, 67, 471
Kızıltan, B., Baumgardt, H., & Loeb, A. 2017a, Natur, 542, 203
Kızıltan, B., Baumgardt, H., & Loeb, A. 2017b, Natur, 545, 510
Kuijken, K., & Gilmore, G. 1989, MNRAS, 239, 605
Latif, M. A., & Ferrara, A. 2016, PASA, 33, e051
Lin, D., Strader, J., Carrasco, E. R., et al. 2018, NatAs, 2, 656
Lugger, P. M., Cohn, H. N., & Grindlay, J. E. 1995, ApJ, 439, 191
Lützgendorf, N., Kissler-Patig, M., Gebhardt, K., et al. 2013, A&A, 552, A49
Lynch, R. S., Freire, P. C. C., Ransom, S. M., & Jacoby, B. A. 2012, ApJ, 745, 109
Manchester, R. N., Hobbs, G. B., Teoh, A., & Hobbs, M. 2005, AJ, 129, 1993
McLaughlin, D. E., Anderson, J., Meylan, G., et al. 2006, ApJS, 166, 249
McNamara, B. J., Harrison, T. E., Baumgardt, H., & Khalaj, P. 2012, ApJ, 745, 175
Mezcua, M. 2017, IJMPD, 26, 1730021

Miller, M. C., & Hamilton, D. P. 2002, MNRAS, 330, 232
Miocchi, P., Lanzoni, B., Ferraro, F. R., et al. 2013, ApJ, 774, 151
Nice, D. J., & Taylor, J. H. 1995, ApJ, 441, 429
Noyola, E., & Gebhardt, K. 2006, AJ, 132, 447
Noyola, E., Gebhardt, K., & Bergmann, M. 2008, ApJ, 676, 1008
Perera, B. B. P., Stappers, B. W., Lyne, A. G., et al. 2017a, MNRAS, 468, 2114
Perera, B. B. P., Stappers, B. W., Lyne, A. G., et al. 2017b, MNRAS, 471, 1258
Portegies Zwart, S. F., Baumgardt, H., Hut, P., Makino, J., & McMillan, S. L. W. 2004, Natur, 428, 724
Portegies Zwart, S. F., & McMillan, S. L. W. 2002, ApJ, 576, 899
Possenti, A., D'Amico, N., Manchester, R. N., et al. 2003, ApJ, 599, 475
Prager, B. J., Ransom, S. M., Freire, P. C. C., et al. 2017, ApJ, 845, 148
Sharma, S., Bland-Hawthorn, J., Binney, J., et al. 2014, ApJ, 793, 51
Shklovskii, I. S. 1970, SvA, 13, 562
Spitzer, L. 1987, Dynamical Evolution of Globular Clusters (Princeton, NJ: Princeton Univ. Press)
Tremou, E., Strader, J., Chomiuk, L., et al. 2018, ApJ, 862, 16
van der Marel, R. P., & Anderson, J. 2010, ApJ, 710, 1063
Volonteri, M. 2010, A&ARv, 18, 279
Watkins, L. L., van der Marel, R. P., Bellini, A., & Anderson, J. 2015, ApJ, 803, 29
Ye, C. S., Kremer, K., Chatterjee, S., Rodriguez, C. L., & Rasio, F. A. 2019, ApJ, 877, 122